Plasmonic Glasses and Films Based on Alternative Inexpensive Materials for Blocking Infrared Radiation

Lucas V. Besteiro,[1,2] Xiang-Tian Kong, [1,3] Zhiming Wang,[1*] Federico Rosei,[2*] Alexander O. Govorov[3*]

[1] *Institute of Fundamental and Frontier Sciences, University of Electronic Science and Technology of China, Chengdu 610054, China*

[2] *Centre Énergie Matériaux et Télécommunications, Institut National de la Recherche Scientifique, 1650 Boul. Lionel Boulet, Varennes, QC J3X 1S2, Canada*

[3] *Department of Physics and Astronomy, Ohio University, Athens OH 45701*

* E-mails: jmwahng@gmail.com; rosei@emt.inrs.ca; govorov@ohio.edu

Abstract: The need for energy-saving materials is pressing. This paper reports on the design of energy-saving glasses and films based on plasmonic nanocrystals that efficiently block infrared radiation. Designing such plasmonic composite glasses is nontrivial and requires to take full advantage of both material and shape-related properties of the nanoparticles. We compute the performance of solar plasmonic glasses incorporating a transparent matrix and specially-shaped nanocrystals. Plasmonic nanoshells are shown to exhibit the best performances as compared to nanorods and nanocups. Simultaneously, the synthesis of plasmonic nanoshells is technologically feasible using gas-phase fabrication methods. The computational work was done for noble metals (gold and silver) as well as for alternative plasmonic materials (aluminum, copper and titanium nitride). Inexpensive plasmonic materials (silver, copper, aluminum and titanium nitride) show overall good performance in terms of the commonly-used figures of merit of industrial glass windows. Together with numerical data for specific materials, this study includes a set of general rules for designing efficient plasmonic IR-blocking media. The plasmonic glasses proposed herein are good candidates for cheap optical media to be used in energy-saving windows in warm climates' housing or temperature-sensitive infrastructure.

1. Introduction

Advanced materials for optical applications are highly desirable in modern technology and industry. An important class of advanced materials consists of optical media for windows, focusing lenses and other related applications. Regarding windows applications, one of the goals is to design an optically-transparent and spectrally-tailored medium that manages and blocks infrared (**IR**)

radiation.[1] The reason for designing such IR-blocking windows lies in reducing the amount of heat transferred to a room or a vehicle and in consequence saving on the energy consumed by AC systems. There are several approaches for making spectrally-selective windows. One approach entails covering a glass with a multi-layered film that reflects IR light, while transmitting the visible part of the solar spectrum.[1–4] Another approach is to use near-IR absorptive materials that can block most of the solar IR radiation.[5] Along with the glasses with static properties, much current interest is now attracted to switchable glasses and windows.[6–8] Certain requirements are imposed on such optical materials: good transmission in the visible range, strong attenuation in the near and short-wavelength IR and strong reflection in the long-wavelength IR interval.[3,4,9,10] The latter is used to reflect non-solar radiative heat coming from the street. So-called low-E (low Emissivity) window panes are designed in this manner.[1,2,9–11] From the above three requirements, it is apparent that the decoupling of the visible and IR properties of a glass is crucial to create windows with high performance. A variety of online resources provide useful introductions to the current practices and figures of merit employed in an industrial setting.[9,10,12]

In this paper, we propose a new approach to create IR-blocking glasses. We show that mixtures of specially-shaped plasmonic nanocrystals made of noble (Ag and Au) and alternative materials (TiN, Al, and Cu) can efficiently block IR solar radiation. In particular, nanocrystals of relatively inexpensive plasmonic materials (Ag, Cu, Al and TiN) show overall good performance as IR-blocking elements. In our approach, a metaglass incorporates a mixture of plasmonic nanocrystals (**NCs**) of different sizes. Since each NC exhibits a narrow plasmonic band, a mixture of NCs can be designed to have a spectrum that efficiently covers the near-IR and

short-wavelength IR intervals (Figure 1d). By adjusting the concentrations of NCs and taking suitable sizes, one can construct an absorption spectrum out of narrow plasmonic peaks (Figure 1d). The resulting medium is expected to block the IR light starting from wavelengths of 700 nm (Figure 1d). Simultaneously, the meta-glass should remain transparent in the visible. We show that the most efficient shape for a NC is a complete nanoshell with relatively small width. Other possible shapes for high-performance glasses are nanorods and nanocups. As it is reasonable to expect, spherical NCs are not suitable for this purpose, since they do not offer sharp and easily-designed optical features. The reasons are that the plasmon resonance in spherical NCs is not very tunable with increasing size, also becoming broad for large sizes, and that size increase for spherical geometries involves a greater material volume increase that leads to larger intraband absorption near the visible interval. This metaglass concept is based on the tunability of plasmonic resonances with the shape and size of a NC.[5,13–22] In particular, it is well known from the literature that plasmonic nanoshells and nanocups have shown excellent tunability of plasmon resonances.[17–23]. The advantage of plasmonic NCs as building elements for metaglasses lies in their very large absorption and scattering cross sections and in their narrow and tunable plasmonic resonances. Recently, it was shown[22,24–26] that, with available colloidal plasmonic NCs, one can construct interesting metasolutions with sharp optical features in the IR spectral interval. A particular optical feature modeled and experimentally realized in Refs. [22,24–26] was a narrow transparency window in the IR. In the present study, we propose another application and another optical material system – a metaglass featuring an IR-blocking step-like spectrum. The goal of our study is to design an efficient metaglass for energy-saving windows.

2. Physical principles of blocking solar and non-solar IR radiation

Figure 1 illustrates the principles followed to create a window that simultaneously blocks IR solar light and does not allow non-solar heat from the outside and from the hot pane to penetrate a cold room. As mentioned in the introduction, decoupling the electromagnetic properties in the visible range and in the IR intervals is crucial.[1–4,9,10] Therefore, three distinct spectral intervals should be considered: visible (**Vis**, 390-700nm), near-IR and short-wavelength IR (**NIR** and **SW-IR**; 0.7-3 μm), and mid-wavelength and long-wavelength IR (**MW-IR** and **LW-IR**; 3-15 μm). The Sun radiates mostly in the Vis, NIR and SW-IR intervals, as can be seen in Figure 1c, which shows the fractions of solar energy that falls in the different intervals. This figure naturally emphasizes the importance of the IR interval in solar heating: IR contributes a 53% of the total energy, versus only a 44% of Vis. Of course, the visible radiation also carries energy inside a cold room, but it is desirable to provide illumination which is friendly to the human eye. In window technologies, two types of radiation are considered, solar and non-solar.[1,3,12] Non-solar heat on a hot day comes from all heated objects around a building and their associated radiation spectrum corresponds to temperature ~ 40 ºC (Figure 1c) and to a characteristic wavelength ~ 10 μm (LW-IR interval).

One of the possible window designs capable of blocking both solar and non-solar thermal radiation is a double-pane argon-filled window with an absorbing external pane[1,2,9] (Figure 1a). In this design, the outside pane is a strong absorber of solar IR photons, yet effectively transmits visible light. The panes are separated by argon gas, that has a low thermal conductivity and low convection. Visible solar light (44% of solar radiated energy) penetrates well into the room, while the IR solar radiation (53%) is absorbed strongly by the outside pane. Since the

outside pane absorbs IR photons, it heats up and radiates energy as a black body at ~ 40 ºC. This radiation should not move into the cold room and, therefore, one should add a coating to reflect the MW-IR and LW-IR radiation with wavelength > 3 μm. This coating can be placed in the internal surface of the outside pane (Figure 1a); this reflective coating can be applied using a thin transparent conducting film (typically, indium tin oxide or similar).[1,2,11] In other words, this transparent coating aims to reflect solar and non-solar thermal radiations in the window system (Figures 1a,c,d).

Solar energy, by definition, is the energy coming as direct radiation from the Sun. The Sun's spectrum is well represented by a black body with its surface temperature $T_{sun} = 5778\,\mathrm{K}$,

$$\frac{dI}{d\lambda} = I_{solar}(\lambda)$$
$$I_{solar}(\lambda) = \frac{A_s}{\lambda^5}\frac{1}{e^{\frac{hc}{\lambda k T_{sun}}} - 1} \qquad \textbf{(1)}$$

Another temperature involved in this system is the temperature of the immediate environment on a hot day. We will assume that this temperature is ~ 40 ºC. Correspondingly, the thermal radiation (non-solar) from hot outside objects has the spectrum

$$I_{non-solar}(\lambda) = \frac{A_{ns}}{\lambda^5}\frac{1}{e^{\frac{hc}{\lambda k T_{hot-day}}} - 1},\ T_{hot-day} = 313K.$$

We now introduce the figures of merit of glasses, as used in industry.[2,4,10,11] The first one is the Visible Transmittance (***VT***). This parameter is the fraction of visible light that enters a room through a window,

$$VT = \frac{\int_{390nm}^{700nm} I_{solar}(\lambda)\, T(\lambda)\, d\lambda}{\int_{390nm}^{700nm} I_{solar}(\lambda)\, d\lambda} \qquad \textbf{(2)}$$

where $T(\lambda)$ is the optical transmittance of the window. The next parameter is the IR transmittance (***IRT***):

$$IRT = \frac{\int_{700nm}^{1700nm} I_{solar}(\lambda)\, T(\lambda)\, d\lambda}{\int_{700nm}^{1700nm} I_{solar}(\lambda)\, d\lambda}. \qquad \textbf{(3)}$$

The total energy transmittance of the window for direct solar illumination will be given by the parameter called Solar Heat Gain Coefficient (***SHGC***):

$$SHGC = \frac{\int_{200nm}^{1700nm} I_{solar}(\lambda)\, T(\lambda)\, d\lambda}{\int_{200nm}^{1700nm} I_{solar}(\lambda)\, d\lambda}. \qquad \textbf{(4)}$$

In industry, this parameter also includes radiative and non-radiative transfers of heat created by direct sun flux. Here we focus only on the optical properties and, for simplicity, calculate this parameter through the optical transmission.

To have an useful window, the parameter VT should be as high as possible, since a cold room should still receive visible solar light; a perfect window with ideal transmission of the visible has $VT_{ideal} = 1$. Simultaneously, a perfect window should have $IRT_{ideal} = 0$. In the following, we will examine the above figures of merit for the new plasmonic metaglasses designed here, and we will also offer

comparisons with commercial materials. An ideal window should have a transmission $T(\lambda)=1$ for the visible light and $T(\lambda)=0$ outside the visible interval, which results in $SHGC_{ideal}=0.42756$ for the given integration interval in our equations. In real windows, we should aim to have the parameters $SHGC$, and specially IRT, as small as possible, in order to keep the room cool.

In the above integrals, Equations (2-4), we adopted the following limits of integration: 200 nm-1700 nm. This is a wavelength range for which we have reliable information on the different materials' dielectric constants. This range includes most of the UV portion of the solar spectrum and values from the IR tail up to 10% of the total irradiance, resulting in a reliable approximation to the total solar energy spectrum, especially when accounting for the atmospheric absorption of sunlight. To address the UV part of the spectrum, we added TiO_2 NCs to our metafilms, which strongly blocks the UV interval.

3. Models of plasmonic metafilms based on the Beer-Lambert Law

The transmittance of a mixture of NCs in a transparent matrix is given by:

$$T = \frac{I_t}{I_i} = 10^{-OD} \quad \textbf{(5)}$$

where I_i and I_t are the incident and transmitted intensities, respectively. The Beer-Lambert law[27] states that the optical density OD can be calculated as

$$OD = \frac{L_{opt}}{\ln(10)} \sum_i \sigma_i n_i \quad \textbf{(6)}$$

where L_{opt} is the optical path that the light traverses through the metafilm with embedded NCs. The sum index runs through the different types of NCs in an ensemble, and n_i and σ_i are the number concentration and the extinction cross-section of the i-th species, respectively. Since individual NCs in a metafilm are generally anisotropic, the optical extinction σ_i used in Equation (6) should be averaged over all orientations of a NC relative to the incident light.

The electrodynamic calculations that provide the NC extinction data reported herein have been performed within classical electrodynamics, by solving Maxwell's equations. In particular, we used the commercial package COMSOL, based on the Finite Elements Method. Cross-sections of individual NCs were averaged from the set of directional extinctions calculated for six different illumination conditions (along the three main axes and involving two orthogonal linear polarizations of incident light). Then, these averaged cross-sections were used in Equation (6) to calculate the optical density and the transmission.

Local dielectric constants for the materials of interest were taken from the following sources: Ref. [28] for Au, Ag and Cu, Ref. [29] for Al, and Ref. [30] for TiN.

The above formalism is based on the Beer-Lambert law, which takes into account the extinction of ballistic photons from sun rays. Part of this extinction is due to nanoparticle scattering, which can represent a sizeable contribution for large NCs, and opens up the possibility that scattered photons end up traversing the metaglass and entering into the room. To address this scenario, we have estimated the effect of the diffusion of scattered photons through the plasmonic glass, and we have found that this effect is weak for the systems of interest, accounting to a few percentage points only.

Our study concerns metafilms incorporating NCs of the same shape and material. We can, of course, imagine a metafilm comprising NCs of different shapes and materials, as it was suggested and realized in Refs. [24–26]. Or, one can think about a collection of complexes made of interacting excitonic and plasmonic components.[31–35] Molecular aggregates[36] or metal-atom clusters[5] can also be used as strongly absorbing components. Plasmonic media incorporating nanocrystal assemblies can be made active using soft-matter responsive materials as a matrix.[37] Nanotechnology has two efficient techniques to fabricate simple and complex NCs: colloidal chemistry[31,33,38,39] and gas-phase deposition methods.[19–22,40] Several recent papers reported the fabrication of NCs using gas-phase deposition methods; the related NC designs include nanocups,[19,20,22] complex multilayer nanocups[21] and nanoshells.[40]

4. Results for nanocrystals with sharp and tunable plasmonic resonances

4.1 Metaglasses made of nanoshells of Ag, Au, Al, Cu, TiN

Using available experimental data for bulk optical dielectric constants of the plasmonic crystals of interest, we now compute extinctions for a set of illustrative sizes in a few different geometries. Figure 2 shows the typical spectra of nanoshells, in which we use the Ag nanoshell as an illustrative example. Its extinction spectrum has its major peak due to a dipolar plasmon, one minor peak due to a quadrupolar excitation and an UV band appearing due to Ag interband transitions. The major dipolar peak is of main interest for us. The spectra of Ag and Cu nanoshells are given in Figure 2b, whereas the spectra of the other NCs are placed in the Supporting Information.

In the next step, we prepare sets of NCs which can efficiently block solar IR radiation, but do not attenuate in the visible interval. To choose such sets of particles, we should explore a range of material and geometrical properties of nanostructures. As it is well known, and also clear from Figure 2, the plasmon peak of a NC is depends strongly on its size, whereas the interband transitions are not spectrally tunable. Therefore, we need to select the sizes of NCs with plasmon peaks in the IR and, simultaneously, we should choose materials with interband transitions in the UV, to avoid attenuating light in the visible interval when passing through the metaglass. In our case, we keep the shell thickness constant, change the core diameter and sample various suitable material systems. In addition, we include TiO_2 NCs ($a = 10\,\text{nm}$) to block light in the UV interval. Table 1 summarizes the sets NCs that create metafilms with best performances within the given NC size set.

Shape Material	Shells (a, w) (nm): n (m^{-3})	Nanorod (d, L) (nm): n (m^{-3})	Nanocup (a, w) (nm): n (m^{-3})
Ag	TiO_2: $3\cdot10^{21}$ (200, 5): 10^{16}	TiO_2: 10^{20} (10, 38): $2\cdot10^{18}$ (10, 45): 10^{18} (10, 59): 10^{18} (10, 81): $5\cdot10^{17}$ (10, 102): 10^{18}	TiO_2: 10^{21} (150, 14): $3\cdot10^{15}$ (250, 16): $2\cdot10^{15}$
Au	TiO_2: $2\cdot10^{21}$ (50, 5): $3\cdot10^{15}$ (80, 5): $5\cdot10^{15}$ (100, 5): $2\cdot10^{15}$ (180, 5): 10^{15} (200, 5): $5\cdot10^{15}$	TiO_2: 10^{21} (10, 24): $5\cdot10^{17}$ (10, 29): $5\cdot10^{17}$ (10, 38): $5\cdot10^{17}$ (10, 45): $2\cdot10^{17}$ (10, 59): $2\cdot10^{17}$ (10, 81): $2\cdot10^{17}$ (10, 102): $3\cdot10^{17}$	TiO_2: 10^{21} (150, 14): 10^{15} (250, 16): $2\cdot10^{15}$
Al	TiO_2: $2\cdot10^{21}$ (180, 5): $2\cdot10^{15}$ (200, 5): $2\cdot10^{15}$	TiO_2: 10^{21} (10, 102): $4\cdot10^{17}$	TiO_2: 10^{21} (250, 16): $2\cdot10^{15}$
Cu	TiO_2: $3\cdot10^{21}$ (50, 5): $2\cdot10^{15}$ (100, 5): $7\cdot10^{15}$ (200, 5): $5\cdot10^{15}$	TiO_2: $3\cdot10^{20}$ (10, 29): $5\cdot10^{17}$ (10, 38): $2\cdot10^{16}$ (10, 45): $2\cdot10^{17}$ (10, 59): $2\cdot10^{17}$ (10, 81): 10^{17} (10, 102): $2\cdot10^{17}$	TiO_2: 10^{21} (150, 14): 10^{15} (250, 16): $2\cdot10^{15}$
TiN	TiO_2: $3\cdot10^{21}$ (50, 5): $2\cdot10^{16}$ (80, 5): $2\cdot10^{15}$ (130, 5): $3\cdot10^{15}$ (200, 5): $7\cdot10^{15}$	TiO_2: 10^{21} (10, 29): 10^{18} (10, 45): $7\cdot10^{17}$ (10, 81): $4\cdot10^{17}$	TiO_2: 10^{21} (150, 14): 10^{16}

Table 1. Summary of concentrations of NCs used to calculate the properties of IR blocking metaglasses with a thickness of 4 mm.

Figure 3 is the main result of the study. Since silver has no interband transition in the visible and exhibits very sharp plasmonic resonances, it demonstrates the best performance in our calculations. In fact, silver is already widely used for coatings in window technologies.[1,2] Commercial windows with

multilayer coating, including a layer of silver, can reflect solar IR light, but with the drawback of being relatively expensive. The performance of gold nanoshells is also good, but gold is significantly more expensive. Among the alternative inexpensive materials, copper and TiN perform well, but the hybridized high-energy mode of the Al shell[17] falls over the visible range, making Aluminum a less suitable material in the nanoshell geometry.

4.2 Nanocrystals with various shapes

Using the transmission spectra shown in Figures 3,4 we can see that the nanoshell geometry shows the best performance. To quantitatively compare different materials and shapes, we then computed the figures of merit (see section 2) from the transmissions in Figures 3,4. Figure 5 shows the results, where we see that, among the options considered, the nanoshell is the best shape, and silver is the best material. Copper is also a suitable candidate for applications of this kind, as well as Al nanorods (Figure 5). For comparison, in Figure 5, we also provide parameters of some commercial glasses.[1,10] We see that our plasmonic glasses look very promising and, in fact, may compete with current commercial products. The parameter Vis for the plasmonic metaglasses is slightly lower than those for the commercial glasses with low-E coatings, but plasmonic glasses can be made from cheaper materials (Cu, TiN, and Al). In addition, the parameter SHGC for plasmonic glasses is close to the optical limit.

4.3. The rules to design an IR-blocking spectrum with plasmonic nanocrystals

Finally, we will formulate a set of rules on how to create efficient metaglass designs. By modeling NCs of several district shapes and different plasmonic materials, we observed that, to achieve a high-quality IR blocking barrier, one should follow the following guidelines:

1) Sizes of plasmonic NCs should be as small as possible to obtain sharper plasmon peaks. Small NCs are better since they have plasmonic peaks with no radiative broadening; the width of the plasmonic peak in small NCs in the IR interval is given by the Drude broadening constant of a metal. Yet, we assume here that the NC size should be larger than a few nanometers, to display plasmonic character.
2) Spherical NCs are not very useful. They do not have enough tunability of their plasmon energy. Large spherical NCs have broad peaks (Mie resonances) with a very strong radiative broadening.[41]
3) In the case of nanoshells, one should use shells with small widths. This reduces the total material volume, thus producing a weaker interband absorption in the visible interval.
4) Use materials with interband transitions in the UV range. Such materials may be of a silver-like color.
5) Since the extinction spectrum of a metaglass depends on both plasmonic resonances and interband spectral structures, it is important to sample several NC geometries. For example, Al nanorods have shown a good performance, whereas Al nanoshells were not found particularly suitable.

Regarding the potential applications and fabrication of metafilms, the following remarks apply: (1) Alternative inexpensive materials, such as Cu, TiN or Al are promising. As it was demonstrated above, Cu and TiN nanoshells can create IR-blocking glasses with an overall good performance. Also, Al nanorods offer

decent values for figures of merit. (2) Gas-phase templated deposition using polymer and glass nanospheres allows to fabricate nanoshells and nanocups with variable sizes.[19,21,22,40] Therefore, nanoshells and nanocups seem to be the most technologically accessible shapes.

Conclusions

We have studied the possibility of designing IR-blocking glasses using plasmonic NCs. While it is certainly tempting to use plasmonic elements for managing light, there are some challenges to their implementation, of economical, technological and fundamental nature. For such applications, one should use relatively inexpensive plasmonic materials. In particular, we have shown that NCs made of silver, copper, aluminum and titanium nitride can form plasmonic glasses with high performance, comparable to current commercial energy-saving windows. Technologically, one should be able to fabricate a set of NC with sizes capable of blocking the solar IR range. Recent publications on templated gas-phase deposition techniques have demonstrated that this goal is achievable. Finally, the interband transition bands in the plasmonic materials impose fundamental limitations on the creation of sharp transmission windows for the visible interval. Nevertheless, using rational designs, it is possible to overcome this limitation. By exploring a range of candidate materials and geometries for the embedded plasmonic NCs, we have mapped the metaglass design space for several promising shapes and material systems, and, in doing so, we have sketched guidelines to keep charting it with additional types of NCs. To conclude, we have shown that the metaglass concept is indeed promising for practical applications and can provide a potentially cheaper alternative to the currently used window panes with

a reflective multilayer structure including at least one layer of noble metal (mainly Silver).[1]

The work presented here can be extended in several directions. Most straightforwardly, examining mixed metaglass designs, with different materials and geometries combined in the same pane, as they can provide improved optical properties. Additionally, further sampling of cheap materials and additional NC geometries can provide improved efficiency-to-cost ratios. Other approaches can change the target transmission spectra of the metaglass to, e.g. one that affords specifically colored windows. Overall, the main result achieved in our study is a demonstration that transparent media with specially-selected embedded plasmonic NCs can function as materials for windows with enhanced electromagnetic properties.

Supporting Information

Supporting Information, with additional data, is offered in this same file.

Acknowledgements

L.V.B. was supported by China Postdoctoral Science Foundation and National Natural Sciences Foundation of China (project 51272038). This work was supported by Volkswagen Foundation and by the EU RISE project 734690-SONAR (A.O.G.). A.O.G. and F.R. are Chang Jiang (Yangtze River) Chair Professors of the Government of China. F.R. is grateful to the Canada Research Chairs program for partial salary support. F.R. also acknowledges Sichuan Province for a 1,000 talent short term award.

References

[1] J. Carmody, S. Selkowitz, L. Heschong, *Residential windows: a guide to new technologies and energy performance*; 1st. ed.; Norton: New York, 1996.
[2] F. Pacheco-Torgal, *Eco-efficient materials for mitigating building cooling needs*; Elsevier: Boston, MA, 2015.
[3] J. A. Duffie, W. A. Beckman, *Solar engineering of thermal processes*; 4th ed.; John Wiley: Hoboken, 2013.
[4] *Advances in passive cooling*; Santamouris, M., Ed.; Buildings, energy, solar technology; Earthscan: London ; Sterling, VA, 2007.
[5] T. K. N. Nguyen, A. Renaud, M. Wilmet, N. Dumait, S. Paofai, B. Dierre, W. Chen, N. Ohashi, S. Cordier, F. Grasset, T. Uchikoshi, *J Mater Chem C* **2017**, *5*, 10477.
[6] R. Baetens, B. P. Jelle, A. Gustavsen, *Sol. Energy Mater. Sol. Cells* **2010**, *94*, 87.
[7] D. Wolfe, K. W. Goossen, *Opt. Express* **2018**, *26*, A85.
[8] S. Haghanifar, T. Gao, R. T. Rodriguez De Vecchis, B. Pafchek, T. D. B. Jacobs, P. W. Leu, *Optica* **2017**, *4*, 1522.
[9] What When How, Window energy.
[10] Seven Sun Windows, Insulating Glass.
[11] E. Hammarberg, A. Roos, *Thin Solid Films* **2003**, *442*, 222.
[12] Glass Knowledge Blog, Non-solar heat control glasses.
[13] S. A. Maier, *Plasmonics: fundamentals and applications*; Springer: New York, 2007.
[14] *Complex-shaped metal nanoparticles: bottom-up syntheses and applications*; Murphy, C. J.; Sau, T. K.; Rogach, A. L., Eds.; Wiley-VCH: Weinheim, 2012.
[15] C. L. Haynes, R. P. Van Duyne, *J. Phys. Chem. B* **2001**, *105*, 5599.
[16] A. Joplin, W.-S. Chang, S. Link, *Langmuir* **2017**.
[17] E. Prodan, C. Radloff, N. J. Halas, P. Nordlander, *Science* **2003**, *302*, 419.
[18] M. G. Blaber, M. D. Arnold, M. J. Ford, *J. Phys. Chem. C* **2009**, *113*, 3041.
[19] J. Ye, N. Verellen, W. Van Roy, L. Lagae, G. Maes, G. Borghs, P. Van Dorpe, *ACS Nano* **2010**, *4*, 1457.
[20] P. Van Dorpe, J. Ye, *ACS Nano* **2011**, *5*, 6774.
[21] M. Frederiksen, V. E. Bochenkov, M. B. Cortie, D. S. Sutherland, *J. Phys. Chem. C* **2013**, *117*, 15782.

[22] Y. Qin, X.-T. Kong, Z. Wang, A. O. Govorov, U. R. Kortshagen, *ACS Photonics* **2017**, *4*, 2881.
[23] H. Wang, Y. Wu, B. Lassiter, C. L. Nehl, J. H. Hafner, P. Nordlander, N. J. Halas, *Proc. Natl. Acad. Sci.* **2006**, *103*, 10856.
[24] H. Zhang, H. V. Demir, A. O. Govorov, *ACS Photonics* **2014**, *1*, 822.
[25] L. V. Besteiro, K. Gungor, H. V. Demir, A. O. Govorov, *J. Phys. Chem. C* **2017**, *121*, 2987.
[26] J. Yang, N. J. Kramer, K. S. Schramke, L. M. Wheeler, L. V. Besteiro, C. J. Hogan, A. O. Govorov, U. R. Kortshagen, *Nano Lett.* **2016**, *16*, 1472.
[27] J. D. Ingle, S. R. Crouch, *Spectrochemical analysis*; Prentice Hall: Englewood Cliffs, N.J, 1988.
[28] P. B. Johnson, R. W. Christy, *Phys. Rev. B* **1972**, *6*, 4370.
[29] A. D. Rakić, *Appl. Opt.* **1995**, *34*, 4755.
[30] U. Guler, A. Kildishev, A. Boltasseva, V. Shalaev, *Faraday Discuss* **2014**.
[31] G. P. Wiederrecht, G. A. Wurtz, J. Hranisavljevic, *Nano Lett.* **2004**, *4*, 2121.
[32] W. Zhang, A. O. Govorov, G. W. Bryant, *Phys. Rev. Lett.* **2006**, *97*, 146804.
[33] B. G. DeLacy, O. D. Miller, C. W. Hsu, Z. Zander, S. Lacey, R. Yagloski, A. W. Fountain, E. Valdes, E. Anquillare, M. Soljačić, S. G. Johnson, J. D. Joannopoulos, *Nano Lett.* **2015**, *15*, 2588.
[34] X. Zhou, J. Wenger, F. N. Viscomi, L. Le Cunff, J. Béal, S. Kochtcheev, X. Yang, G. P. Wiederrecht, G. Colas des Francs, A. S. Bisht, S. Jradi, R. Caputo, H. V. Demir, R. D. Schaller, J. Plain, A. Vial, X. W. Sun, R. Bachelot, *Nano Lett.* **2015**, *15*, 7458.
[35] I. M. Soganci, S. Nizamoglu, E. Mutlugun, O. Akin, H. V. Demir, *Opt. Express* **2007**, *15*, 14289.
[36] S. K. Saikin, A. Eisfeld, S. Valleau, A. Aspuru-Guzik, *Nanophotonics* **2013**, *2*.
[37] L. De Sio, R. Caputo, U. Cataldi, C. Umeton, *J. Mater. Chem.* **2011**, *21*, 18967.
[38] J. Zhang, Y. Tang, K. Lee, M. Ouyang, *Nature* **2010**, *466*, 91.
[39] L. Weng, H. Zhang, A. O. Govorov, M. Ouyang, *Nat. Commun.* **2014**, *5*, 4792.
[40] K. Manandhar, J. A. Wollmershauser, B. N. Feigelson, *J. Vac. Sci. Technol. Vac. Surf. Films* **2017**, *35*, 041503.
[41] S. Asano, G. Yamamoto, *Appl. Opt.* **1975**, *14*, 29.

Figures

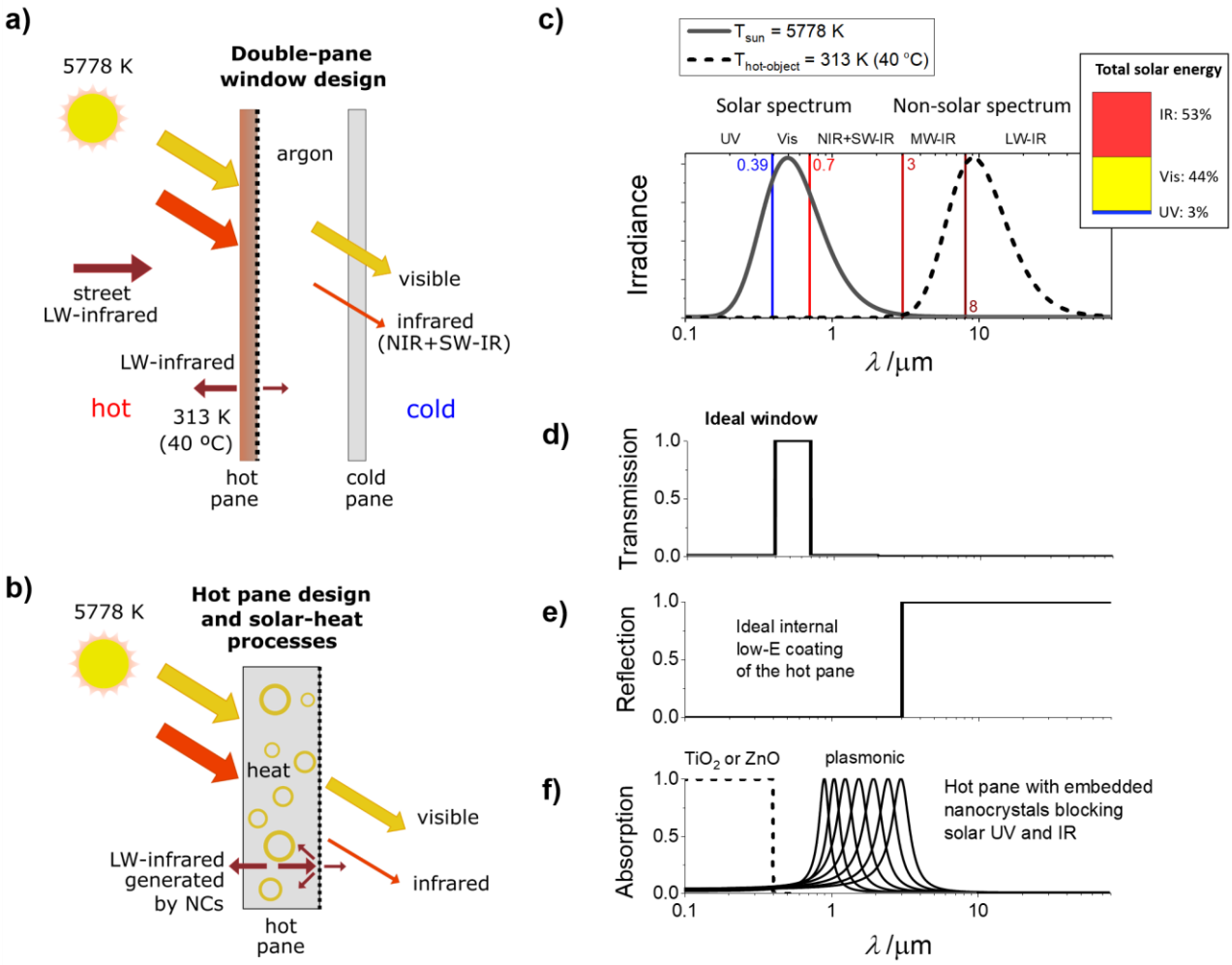

Figure 1. Elements of energy-saving windows and related optical properties and characteristics. **a)** The structure of a commercial double-pane argon window.[9,10] The front pane absorbs the solar IR and, in addition, has a low-E coating on the internal surface for reflection of non-solar thermal radiation (mid- and short-wavelength IR, **MW-IR** and **SW-IR** radiation) coming from hot objects in the street and from the hot external window pane itself. **b)** Illustration of a metafilm incorporating a transparent matrix (glass) and a collection of plasmonic nanocrystals of different sizes. **c)** Black-body spectrum of the Sun and a hot outside temperature (40 ºC). **d)** Spectral characteristics of an ideal IR-blocking and low-E window. The outside hot pane has embedded semiconductor and plasmonic

nanocrystals that block the solar ultraviolet (**UV**) and IR radiation. **e)** Reflection spectrum of an ideal low-E coating on the internal surface of the hot pane. **f)** Schematics of the absorption spectra of plasmonic nanocrystals to cover the NIR and SW-IR intervals and the semiconductor NCs to block the UV interval.

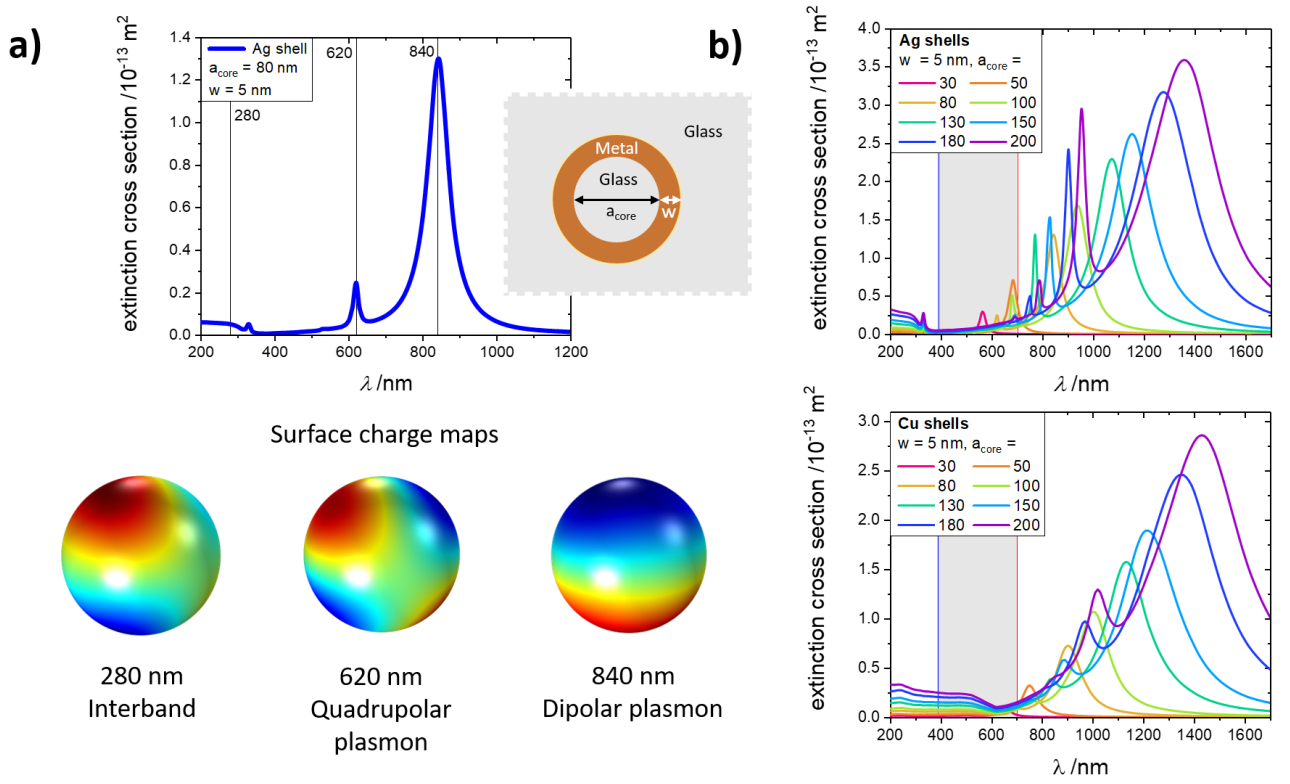

Figure 2. **a)** Ag shell (80 nm, 5 nm) and its external surface charges, accompanied by a diagram of the central slice of a metallic nanoshell with its geometrical parameters. **b)** Calculated extinctions of the set of Ag and Cu nanoshells.

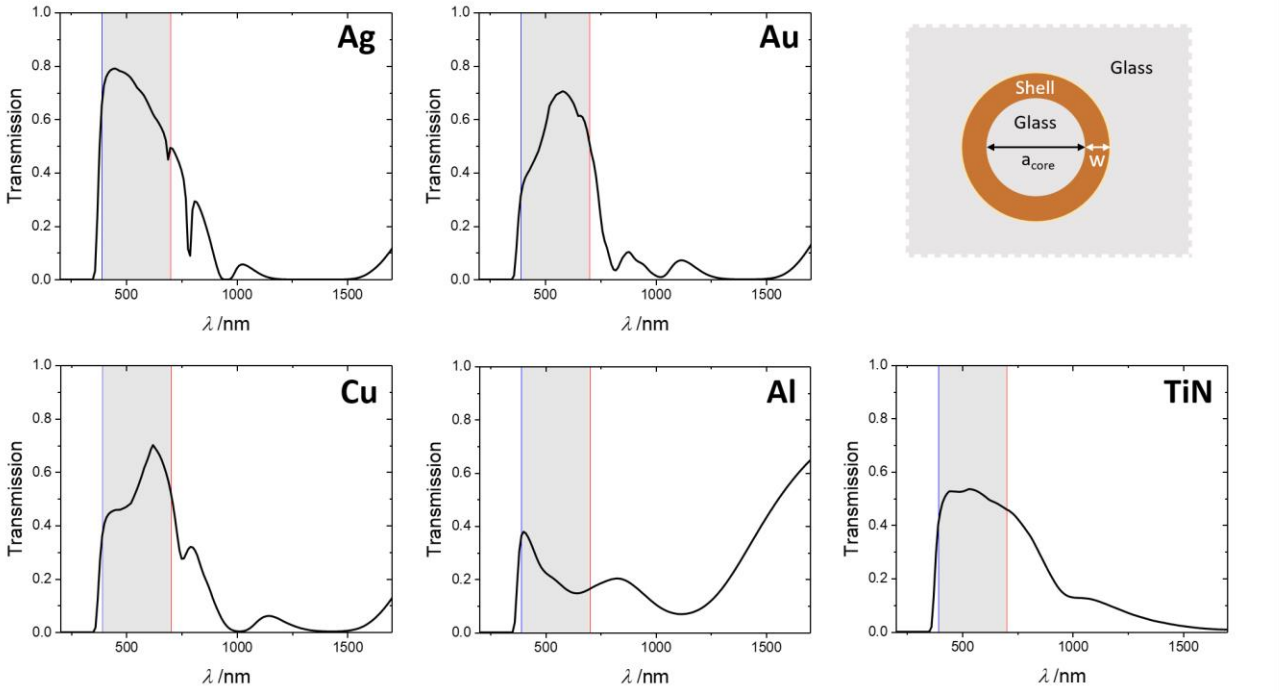

Figure 3. Transmission profiles for glasses embedded with different ensembles of nanoshells. Each different profile has been obtained with nanoshells of only one material. The specific concentrations of different nanoshell sizes in each ensemble can be found in Table 1. The diagram shows a schematic slice of a nanoshell.

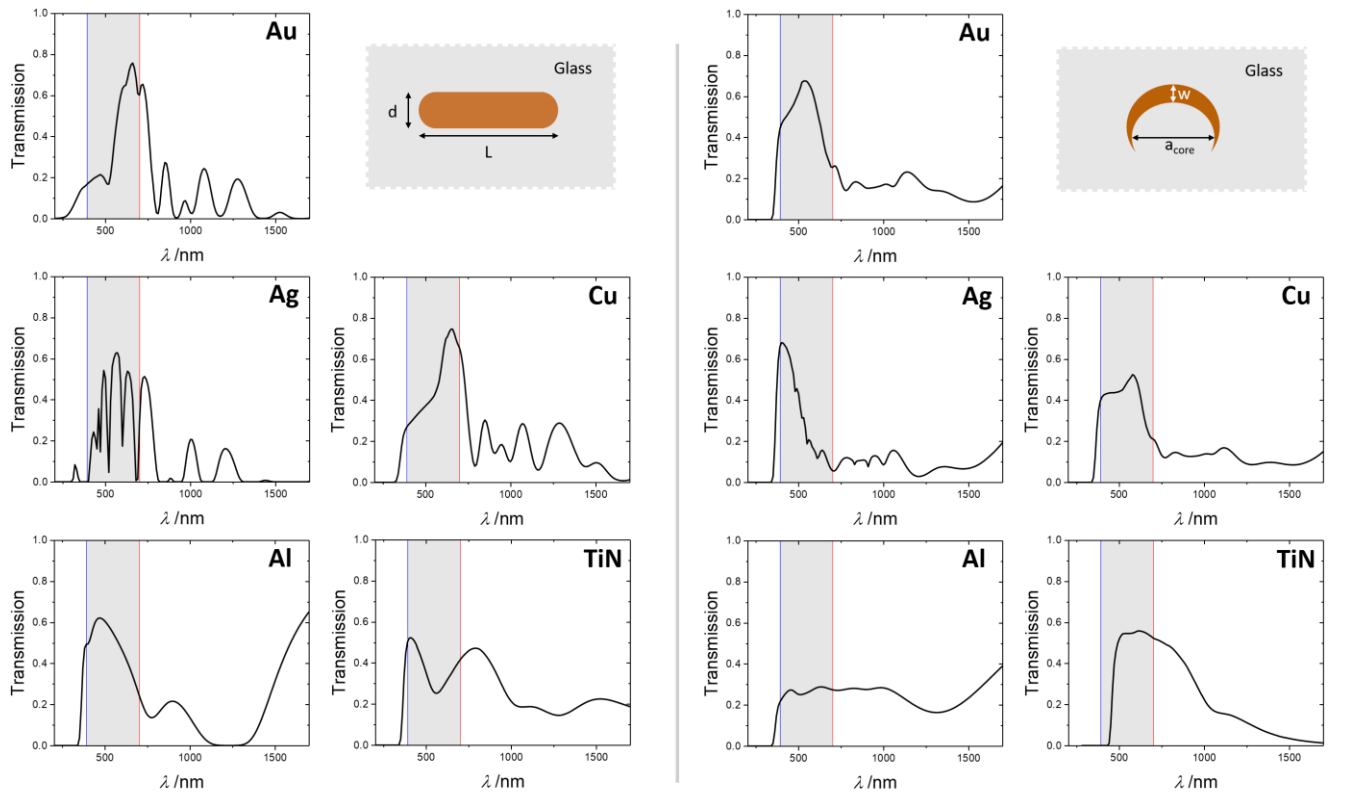

Figure 4. Transmission profiles for glasses embedded with different ensembles of nanorods (left) and nanocups (right). Each different profile has been obtained with NCs of only one material. The specific concentrations of different NC sizes in each ensemble can be found in Table 1. The diagrams show a schematic slice of a nanorod and a nanocup, respectively.

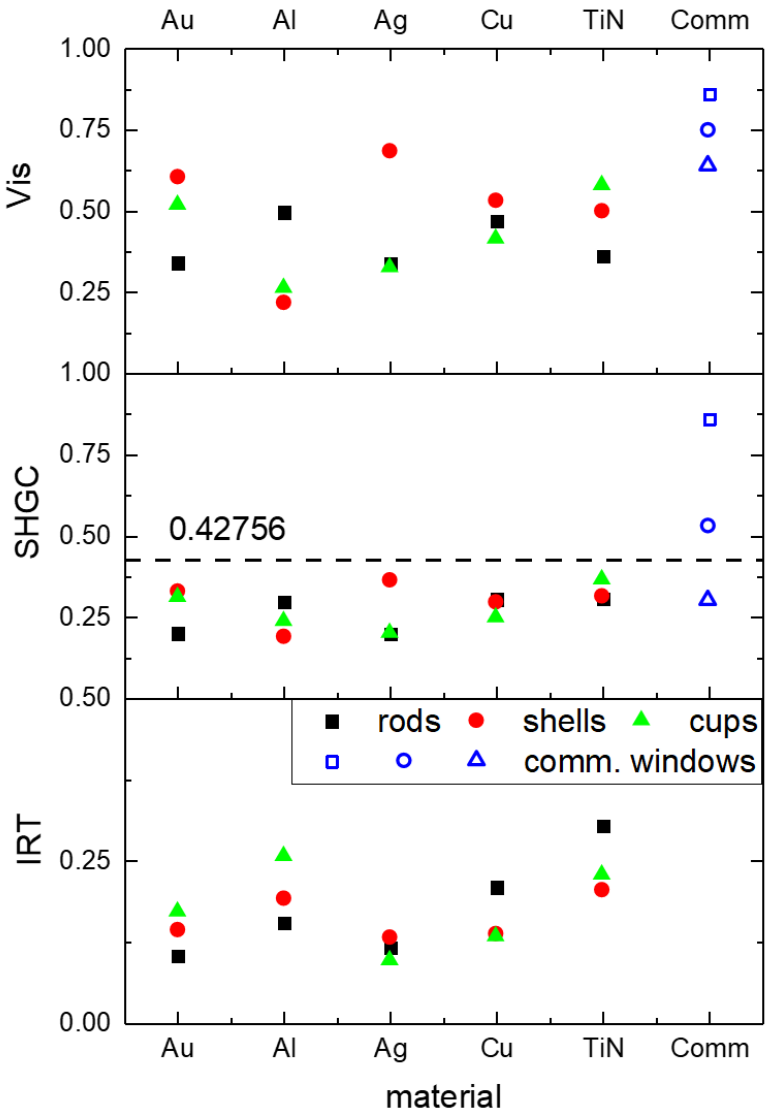

Figure 5. Figures of merit for various plasmonic IR-blocking glasses and also for commercial windows. Interestingly, some of the proposed plasmonic systems achieve a close-to-ideal SHGC parameter, although the parameters VT and IRT are not ideal (VT < 1 and IRT > 0), as it is also the case with commercial windows. In this graph, the parameters for commercial windows were taken from the literature. We looked at three cases: window 1 (hollow square) - single-pane clear glass;[10] window 2 (hollow circle) - double pane argon Low-E coating;[1] window 3 (hollow triangle) - double pane argon Low-E coating.[10] Metaglass data is obtained for the concentrations given in Table 1.

Supplementary Information

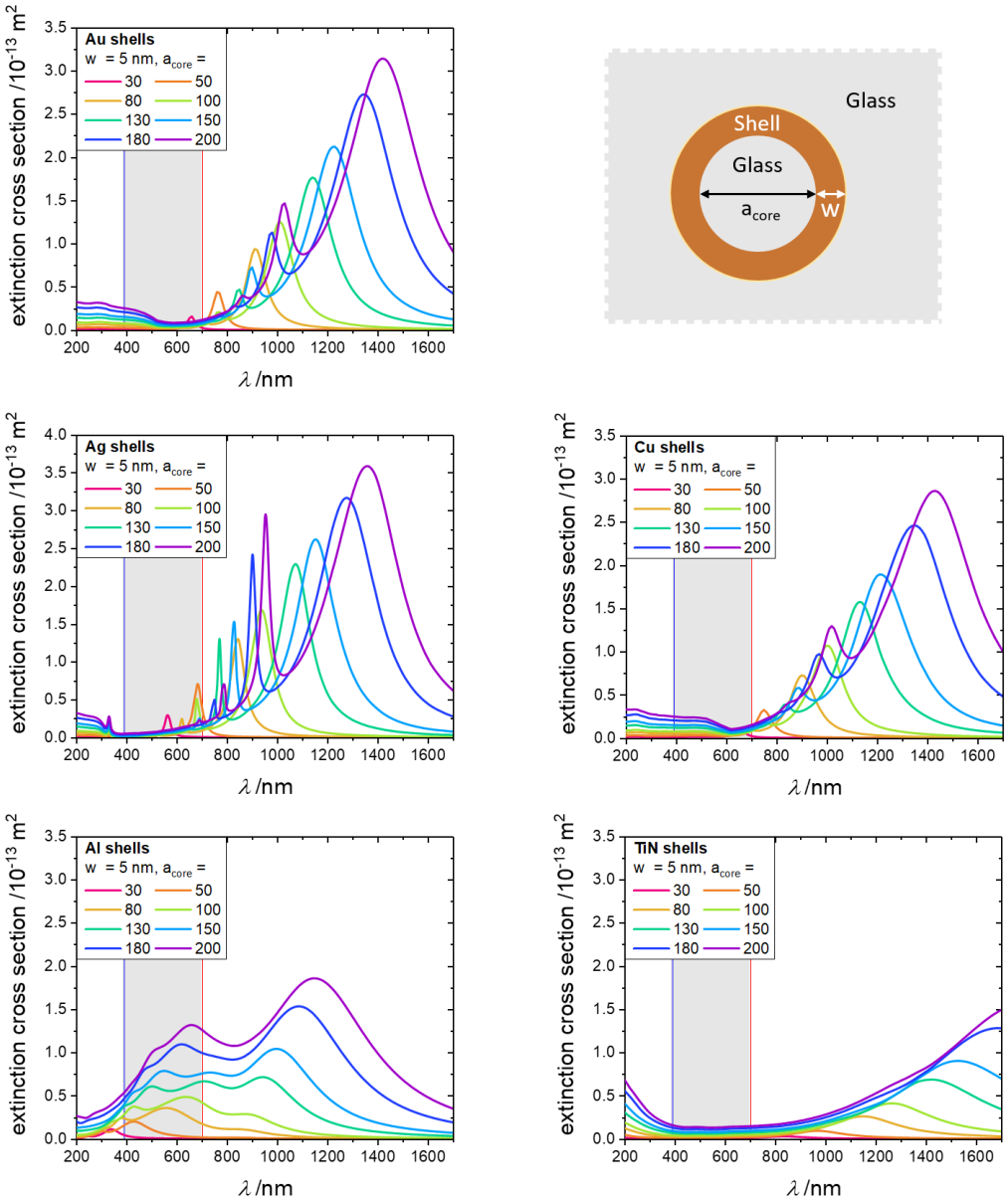

Figure S1. Extinction cross sections of the ensemble of nanoshell sizes considered in our calculations, grouped by material. Note that the proposed metaglasses (Figure 3) use different concentrations of each NC size, as described in Table 1.

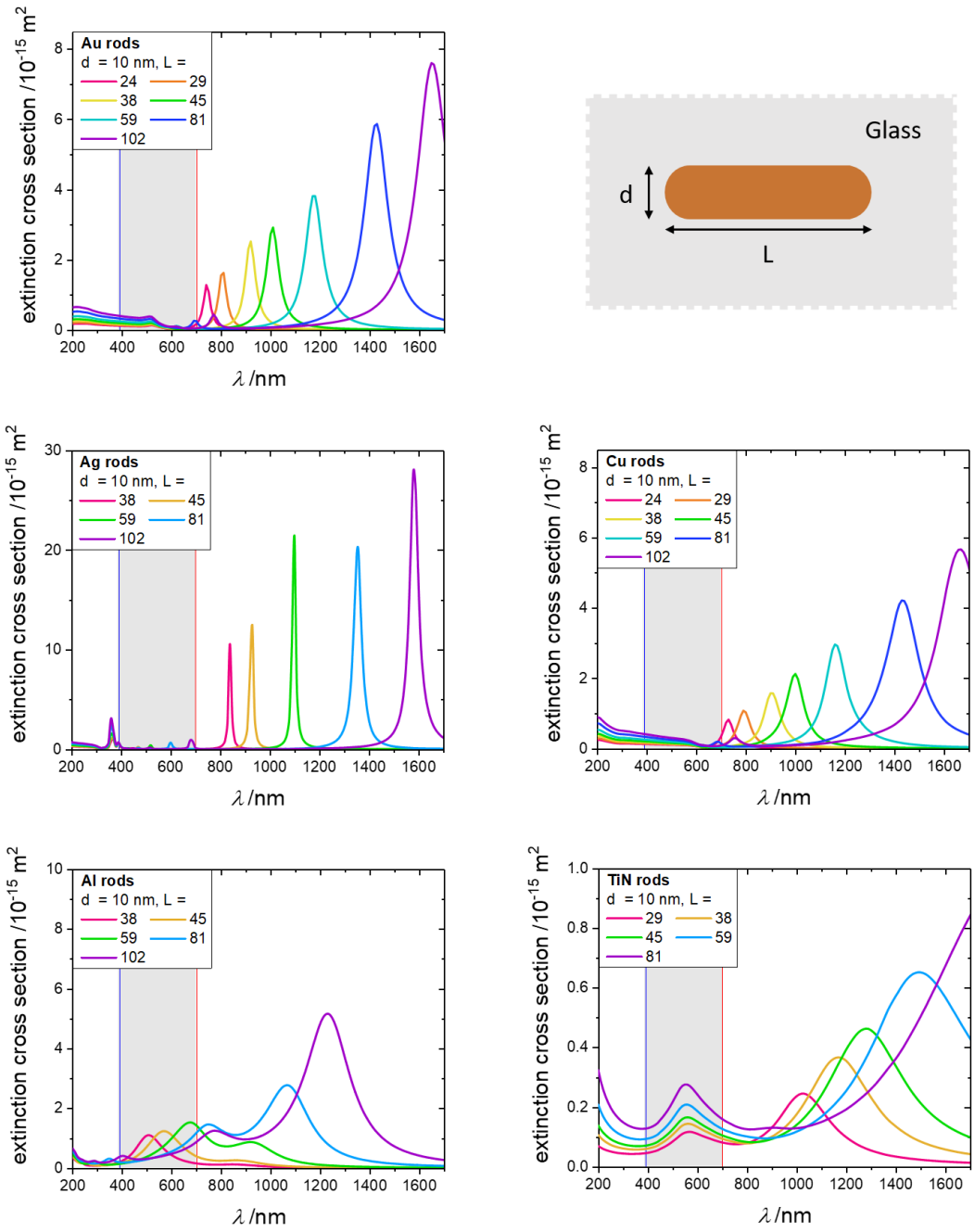

Figure S2. Extinction cross sections of the ensemble of nanorod sizes considered in our calculations, grouped by material. Note that the proposed metaglasses (Figure 4) use different concentrations of each NC size, as described in Table 1.

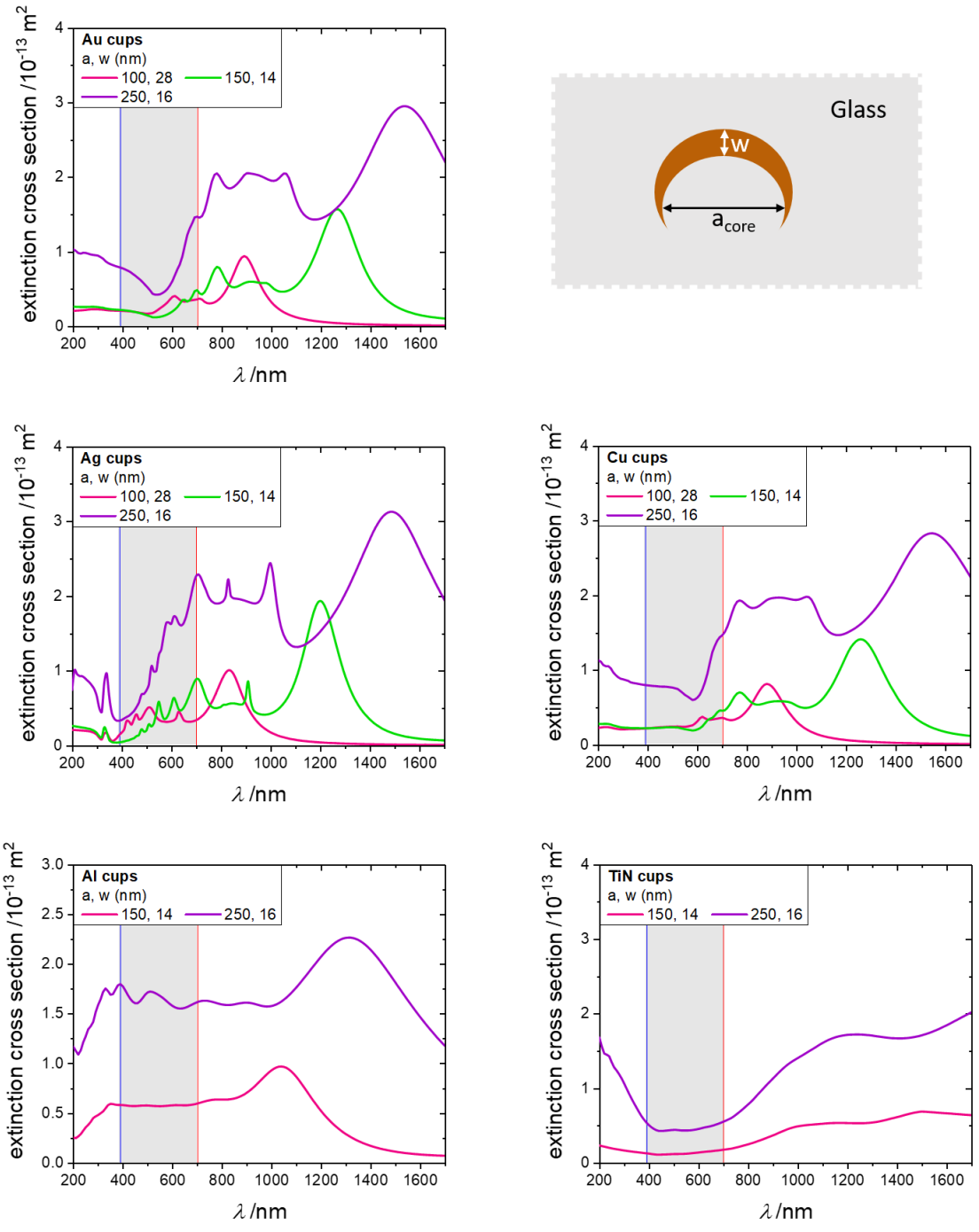

Figure S3. Extinction cross sections of the ensemble of nanocup sizes considered in our calculations, grouped by material. Note that the proposed metaglasses (Figure 4) use different concentrations of each NC size, as described in Table 1.